Nuclear Instruments and Methods in Physics Research B 365 (2015) 482–489

Contents lists available at ScienceDirect

Nuclear Instruments and Methods in Physics Research B

journal homepage: www.elsevier.com/locate/nimb

Time-of-flight secondary neutral & ion mass spectrometry using swift heavy ions

L. Breuer [a], F. Meinerzhagen [a], M. Bender [b], D. Severin [b], A. Wucher [a,*]

[a] Universität Duisburg-Essen, Fakultät für Physik, D-47048 Duisburg, Germany
[b] Gesellschaft für Schwerionenforschung GSI, D-64291 Darmstadt, Germany

ARTICLE INFO

Article history:
Received 8 June 2015
Received in revised form 20 July 2015
Accepted 28 July 2015
Available online 14 September 2015

Keywords:
Electronic sputtering
Ionization probability
Post-ionization
MeV-SIMS
MeV-SNMS

ABSTRACT

We report on a new time-of-flight (TOF) spectrometer designed to investigate sputtering phenomena induced by swift heavy ions in the electronic stopping regime. In this experiment, particular emphasis is put on the detection of secondary ions along with their emitted neutral counterparts in order to examine the ionization efficiency of the sputtered material. For the detection of neutral species, the system is equipped with a pulsed VUV laser for post-ionization of sputtered neutral atoms and molecules via single photon ionization at a wavelength of 157 nm (corresponding to 7.9 eV photon energy). For alignment purposes and in order to facilitate comparison to nuclear sputtering conditions, the system also includes a 5 keV Ar^+ ion beam directed to the same sample area. The instrument has been added to the M1-branch beam line at the German accelerator facility in Darmstadt (GSI) and was tested with 4.8 MeV/u Au^{26+} ions impinging onto various samples including metals, salts and organic films. It is found that secondary ion and neutral spectra obtained under both bombardment conditions can be acquired in an interleaved manner throughout a single accelerator pulse cycle, thus making efficient use of valuable beam time. In addition, the keV ion beam can be intermittently switched to dc mode between subsequent data acquisition windows and accelerator pulses in order to ensure reproducible surface conditions. For the case of a dynamically sputter cleaned metal surface, comparison of secondary ion and neutral signals obtained under otherwise identical instrumental conditions reveals a nearly identical ionization probability of atoms emitted under electronic and nuclear sputtering conditions.

1. Introduction

If an energetic ion impinges onto a solid surface, it will transfer energy to the solid via collisions with the target atoms (”nuclear stopping”) or electronic excitations (”electronic stopping”). While nuclear stopping dominates at low impact energies, electronic stopping represents the dominant energy loss experienced by a swift heavy ion with MeV/u kinetic energy. One way or the other, part of the deposited energy will be utilized to energize a small volume around the impact point to such an extent that surface particles (atoms or molecules) can be emitted into the vacuum (”sputtering”). It is a well known fact that a large fraction – and often the majority – of the sputtered particles leave the surface as neutrals, and only a rather small fraction is emitted as ions. These secondary ions can be easily detected and selected according to their mass, which is utilized in secondary ion mass spectrometry as a well known surface analysis technique. In this context, a crucial quantity is the ionization probability of a sputtered particle which may depend in a complicated way on the nature of the sputtered species, the sputtering process as well as the nature and chemical state of the surface, leading to a severe problem regarding the quantitation of measured secondary ion mass spectra. Therefore, a rather large body of experimental and theoretical work has been devoted to measure and describe the ionization probability of a sputtered particle (see [1–4] for a few reviews) under nuclear sputtering conditions. As of today, however, reliable experimental data on ionization probabilities of material emitted in the electronic sputtering regime is still scarce, and to the best of our knowledge there is no theoretical ionization model available to predict this quantity.

Sputtering phenomena induced by swift heavy ion impact are often described in terms of the two temperature thermal spike model [5]. At first, the projectile deposits energy into the electronic system of the solid, which is assumed to quickly equilibrate and parametrized by an elevated local electron temperature. Energy transfer to the nuclei is then assumed to occur via electron–phonon coupling, and the energy dynamics within the electronic

* Corresponding author.
E-mail address: andreas.wucher@uni-due.de (A. Wucher).

http://dx.doi.org/10.1016/j.nimb.2015.07.117
0168-583X/

and the nuclear system are treated in terms of two coupled heat conduction equations with a coupling term including the temperature difference and a parametrized coupling constant. On the experimental side, sputter yields (i.e., the number of ejected target atoms per projectile impact) have been measured by means of catcher techniques, where the sputtered material is collected on a catcher foil which is then analyzed using a suitable surface/thin film analysis technique such as Rutherford Backscattering to determine the amount of deposited material (for an overview, see [5] and references therein). Using the same technique, angular emission distributions have been measured as well [6]. Since these techniques sample the entire sputtered material, they cannot distinguish between different ejected species such as, for instance, atoms and molecules or clusters of the same element. The ionized fraction of the sputtered material, on the other hand, is readily available for mass spectrometric analysis and can therefore be utilized to investigate the composition of the sputtered flux. What remains unclear, is (i) what fraction of the sputtered particles is ejected in ionized form and (ii) how that fraction depends on parameters like nature and impact energy of the projectiles, nature and chemical state of the target material etc. Using a quadrupole mass spectrometer, Rothard et al. [7] addressed the first question by comparing the total secondary ion yield, Y_+, measured this way to the total sputter yield, Y_{tot}, measured by a catcher foil. While this method delivers the average ion fraction of the sputtered material, it cannot provide mass specific information about the ionization probability of different ejected particles. For that purpose, mass resolved information about the neutral particle flux emerging from the surface is needed. These particles, on the other hand, need to be post-ionized subsequent to their emission in order to render them detectable in a mass spectrometer, and extreme care must be taken in order to ensure that the post-ionization process does not falsify the result. To our knowledge, no attempt to collect such information for particles emitted in the electronic sputtering regime has been made to date. In our group, we have developed a method based on laser post-ionization of sputtered neutrals, where secondary ions and neutrals are being detected in situ under otherwise identical experimental conditions. In the present paper, we describe an approach to utilize this technique for the investigation of sputtering phenomena under bombardment of different materials with swift heavy ions (SHI). More specifically, a time-of-flight (TOF) mass spectrometer was installed at the M-branch of the UNILAC beam line at GSI (Darmstadt, Germany) and combined with a VUV laser for post-ionization of sputtered neutral species. Here, we report on first results obtained with this setup regarding the ionization probability of metal atoms sputtered under bombardment with 4.8 MeV/u Au^{26+} ions.

2. Experimental

The experiments were carried out at the M1-branch of the UNILAC beam line at GSI, which delivers a pulsed ion beam of selectable ion species and energy into an ultrahigh vacuum irradiation chamber connected to a secondary chamber for sample introduction, preparation and analysis as described in detail elsewhere [8]. A home-built TOF spectrometer described in detail elsewhere [9,10] was added to the analysis chamber under an angle of 45° with respect to the SHI beam direction. The sample is mounted to a programmable stage and positioned in such a way that the surface is perpendicular to the ion optical axis of the TOF spectrometer and the SHI beam impinges under 45° with respect to the surface normal. The scheme of the setup is depicted in Fig. 1. The investigated surface is bombarded with either a pulsed Ar^+ ion beam with a kinetic energy of typically 5 keV or the SHI beam delivered by the UNILAC. During the primary ion bombardment,

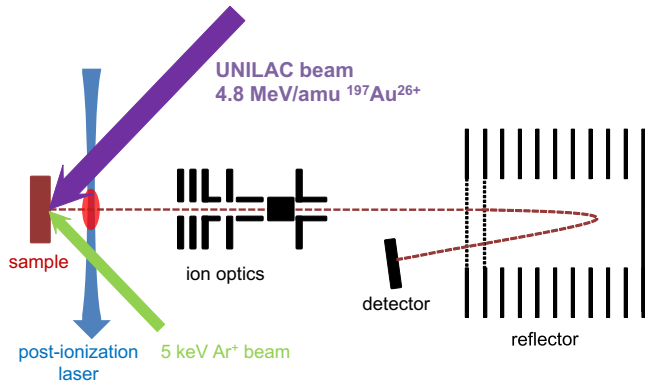

Fig. 1. Schematic setup of reflectron TOF-Mass Spectrometer with laser post-ionization for combined SIMS/SNMS measurements. Red area: sensitive volume probed by the mass spectrometer. (For interpretation of the references to color in this figure legend, the reader is referred to the web version of this article.)

the sample is kept at ground potential and the space between the surface and the extraction electrode is field-free. Sputtered secondary particles (ions as well as neutrals) therefore freely expand according to their emission velocity distribution into the vacuum above the surface. To render secondary neutral particles detectable, they are post-ionized via non-resonant single photon ionization using a focused laser beam of $\lambda = 157$ nm and a photon energy of $h\nu = 7.9$ eV. Secondary ions as well as post-ionized secondary neutral particles are then extracted into the mass spectrometer by means of a pulsed extraction field which is generated by rapidly switching the sample potential to high voltage. As described in detail elsewhere [11,12], this procedure ensures that secondary ions and the corresponding neutral counterparts are being detected under otherwise identical experimental conditions regarding the probed emission velocity and solid angle interval as well as the transmission and detection efficiency of the TOF mass spectrometer. In the following, we will refer to spectra acquired with the post-ionization laser fired as Secondary Neutral Mass Spectra (SNMS), while those measured without the post-ionization laser will be referred to as Secondary Ion Mass Spectra (SIMS).

A commercially available excimer laser (ATLEX 500-L, ATL Lasertechnik GmbH) is used to produce pulses of 157 nm wavelength with a pulse duration of 5–8 ns (FWHM) and pulse energies up to 1.7 mJ. Since 157 nm radiation is not transmitted through air, an evacuated beam line connects the laser to the vacuum chamber via an adjustable mirror. A CaF_2 lens (focal length 20.9 cm) is used to steer and focus the beam into the sensitive volume of the mass spectrometer, which is determined by the ion optical properties of the reflectron spectrometer and set to be located about 1 mm above the sample surface. With a controlled delay after the ion-impact and the laser pulse, the ion extraction field is switched on and secondary ions as well as post-ionized neutral species present in the sensitive volume are swept into the mass spectrometer and focused onto a chevron-stack MCP-detector both in space and time.

The laser intensity is a crucial parameter for the post-ionization process and therefore needs to be monitored. For that purpose, a photoelectric detector is installed in the analysis chamber which is described elsewhere [8,10,13]. In principle, it is desirable to use a laser intensity that is high enough to drive the post-ionization process into saturation across the entire sensitive volume sampled by the mass spectrometer. While this condition can often be achieved with a more powerful laser installed in our lab (delivering up to 12 mJ/pulse), it is generally not reachable at the UNILAC beam line due to space restrictions limiting the size

and beam geometry of the laser employed here. Therefore, the post-ionization efficiency cannot always be assessed quantitatively. In order to still determine ionization probabilities for secondary particles sputtered under SHI impact, we compare the SIMS and SNMS signals generated by the UNILAC ion beam with those generated with a reference keV ion beam impinging under the same impact angle onto the same surface area. For that purpose, the system is equipped with a rare gas ion source (Leybold IQ100) delivering a beam of 5 keV Ar^+ ions with a beam current of about 100 nA into a spot of about 3 mm diameter.

Alignment of the two beams on the sample surface was performed by means of a chromium-doped Al_2O_3 target, which fluoresces under ion bombardment and allows to take an optical image of the irradiated spot. First, the keV beam was steered such as to maximize the detected secondary ion signal, thereby assuring that the irradiated surface area was centered around the ion optical axis of the mass spectrometer. Then, the UNILAC beam was apertured to irradiate a spot of about 5 mm diameter and steered to overlap with the optical image of the keV beam. Although this way the surface area irradiated by the UNILAC was larger than that irradiated by the keV beam, this does not influence the measured signal, since the surface area probed by the TOF spectrometer is restricted to a diameter of about 1 mm, which was verified by translating the keV beam laterally and monitoring the resulting signal drop.

The timing sequence used in these experiments was optimized in order to make the most efficient use of accelerator beam time. For each sample, spectra were taken with the UNILAC beam, the keV beam and without any ion bombardment. For each bombarding condition, spectra were taken with and without the post-ionization laser in order to differentiate between secondary neutral and ion signals. In order to minimize the amount of beam time, six spectra were therefore acquired in a quasi-simultaneous manner using an interleaved pulsing scheme depicted in Fig. 2. The UNILAC beam is pulsed with a pulse duration of $1\cdots5$ ms and a repetition rate of $1\cdots50$ Hz. These pulses, which are shown in the uppermost row of Fig. 2, are long compared to a typical primary ion pulse width used in a TOF experiment ($\sim$1 μs), so that the beam can be regarded as quasi-continuous during a TOF data acquisition cycle. The flight time resolution therefore results from the fast switching of the extraction field, which sweeps the ions present in the sensitive volume at the switching time into the mass spectrometer. The extraction field remains on for a few microseconds and is then switched off again. Secondary ions emitted directly from the surface during the extraction pulse are not reflected in the mass spectrometer, since the reflector voltage was set slightly below the extraction potential. During the length of an UNILAC pulse, the TOF experiment was repeated as fast as possible, i.e. with a repetition rate of subsequent data acquisition cycles (in the following referred to as "shots") of several kHz. The corresponding extraction pulses, each one representing the acquisition of a TOF spectrum, are depicted in the third row of Fig. 2. Since the laser cannot operate at such a high repetition rate, only the first one of these pulses was routed to trigger the laser (fourth row of Fig. 2), making this shot to contribute to the SNMS spectrum, while the remaining shots contribute to the SIMS spectrum.

In between subsequent UNILAC pulses, additional gates were implemented, during which the blank spectra (without ion bombardment) and the keV spectra (with the keV ion beam on) were acquired. In order to deliver quantitatively comparable information, the duration of the blank gate was adapted to the length of the UNILAC pulse itself. The duration of the keV gate, on the other hand, was made longer in order to accumulate as many shots as possible. Using a rather complicated synchronization protocol, it was made sure that only the first of each shots fired in each gate contributed to the respective SNMS spectrum, while the remaining shots in the same gate contributed to the corresponding SIMS spectrum.

Normally, the laser pulse is fired shortly ($\sim$10 ns) before the extraction is switched on. This way, the instrument cannot distinguish between photoions and secondary ions that were already present before the laser was being fired, so that both species are detected under otherwise identical experimental conditions. In particular, the flight time zero is defined by the switching time of the extraction pulse for both post-ionized neutrals and secondary ions. In some of the experiments, however, the laser pulse was deliberately delayed with respect to the extraction pulse. In that case, the flight time zero for post-ionized species is defined by the timing of the laser pulse, so that secondary ion and neutral spectra are displaced in time and can therefore be distinguished in the measured TOF spectrum. The disadvantage of this technique is that it complicates the interpretation of the measured mass spectrum. On the other hand, the separate detection of secondary ions and post-ionized neutrals allows a detailed comparison of both spectra, as will be shown for sputtered Indium atoms below. Moreover, it allows to identify a possible influence of the post-ionization laser on the secondary ion signals, for instance due to fragmentation or multiple ionization.

As already mentioned in the introduction, the ionization probability of sputtered particles observed under keV ion bombardment is known to critically depend on the chemical state of the surface.

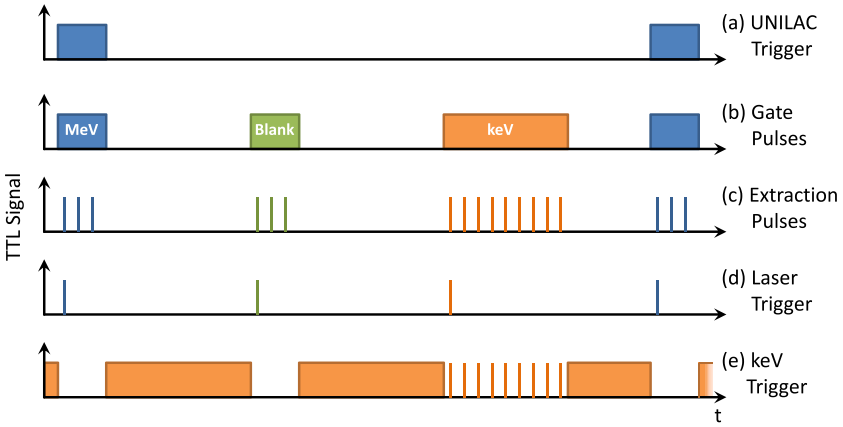

Fig. 2. Interleaved timing scheme used for quasi-simultaneous acquisition of six different mass spectra: MeV-SNMS, MeV-SIMS, keV-SNMS, keV-SIMS, residual gas (with laser only) and Blank.

Therefore, only minor surface contamination can significantly alter the outcome of such a measurement, and it is mandatory to implement a strategy to ensure reproducible surface conditions. In the present experiments, we aim at the determination of ionization probabilities for clean elemental surfaces. The best way to ensure such conditions is to sputter clean the surface with the dc Ar^+ ion beam. Even though all samples were pre-cleaned prior to the analysis by exposing them to the keV beam for several minutes, it was observed that spectra taken after such a pre-cleaning cycle were still influenced by surface contamination building up during the data acquisition. We therefore implemented another interleaving scheme, where the keV ion beam is kept on during all times outside the data acquisition gates as indicated in the bottom row of Fig. 2. This way, the sample is dynamically sputter cleaned with a quasi static ion beam during the entire data acquisition, thus ensuring the cleanest surface condition achievable with the prevailing residual gas pressure. The implication of this is demonstrated for a molybdenum sample in Fig. 3, which shows spectra taken with and without this interleaved sputter cleaning on a surface that was pre-cleaned by dc sputtering for at least 5 min. It is evident that the spectrum taken without the dynamical sputter cleaning is strongly influenced by surface contamination, which manifests in relatively large secondary ion signals and, in addition, abundant molybdenum oxide molecule signals. If the dynamical sputter cleaning is switched on, the secondary ion signals are drastically reduced, while the signal of post-ionized neutral Mo atoms is enhanced, indicating a significant reduction of the surface contamination. Even under these conditions, however, oxide signals are still observed, indicating a residual surface contamination under dc ion beam sputtering which depends on the prevailing vacuum conditions. Note that the SNMS spectra taken with the laser beam and displayed in the left panel reflect the sum of post-ionized neutral and secondary ion signals, whereas the spectra taken without the laser beam and displayed in the right panel correspond to the secondary ions alone. Therefore, it is obvious that a large fraction of the Mo signal and practically all of the MoO and MoO_2 signals detected in the SNMS spectrum without the dynamical cleaning is due to secondary ions, whereas about 90% of the Mo SNMS signal detected with dynamical cleaning is due to sputtered neutral atoms. Remarkably, the spectra obtained without interleaved sputtering were taken after the interleaved sputtering experiment and therefore reflect surface contamination that is building up during the experiment if the dynamical cleaning is switched off.

3. Results and discussion

Besides the fundamental implementation and application of TOF-SIMS/SNMS to investigate the flux of material ejected under electronic sputtering conditions, a primary goal of the present work was to establish a method to determine the ionization probability of the different ejected particles. In the past, our group has devoted a significant effort to determine this quantity for atoms and clusters sputtered from clean elemental surfaces under nuclear sputtering conditions, i.e., using projectile ions with energies in the keV regime. Based on these data, we set out to determine the ionization probability of particles ejected from the same clean elemental surface under electronic sputtering conditions by comparing the spectra measured with the UNILAC beam to reference spectra taken with the keV beam.

In principle, the ionization probability, or, secondary ion formation probability, of a sputtered species can be determined from the signal $S^+ = S_{SIMS}$ and $S^0 = S_{SNMS} - S_{SIMS}$ measured for secondary ions and their neutral counterparts, respectively, as

$$\alpha^+ = \frac{S^+}{cS^0 + S^+} = \frac{S_{SIMS}}{c(S_{SNMS} - S_{SIMS}) + S_{SIMS}}, \quad (1)$$

where the constant c denotes the inverse post-ionization efficiency of the sputtered neutral particles, i.e., $c \geqslant 1$. Although the post-ionization efficiency is unknown in the experiments performed here, its value is independent of the sputtering process, so that Eq. (1) can be written for both keV and MeV sputtering, respectively, and the ratio of ionization probabilities obtained under both sputtering conditions can be written as

$$\frac{\alpha^+_{MeV}}{\alpha^+_{keV}} = \frac{cS^0_{keV}/S^+_{keV} + 1}{cS^0_{MeV}/S^+_{MeV} + 1} \quad (2)$$

In cases where the ionization probability under keV bombardment conditions is known, Eq. (2) can therefore be used to determine its value under SHI bombardment as

$$\alpha^+_{MeV} = \left(\frac{S^{keV}_{SNMS}}{S^{keV}_{SIMS}} - 1\right) \cdot \left[\left(\frac{1}{\alpha^+_{keV}} - 1\right)\frac{S^{MeV}_{SNMS}}{S^{MeV}_{SIMS}} + 1\right]^{-1} \quad (3)$$

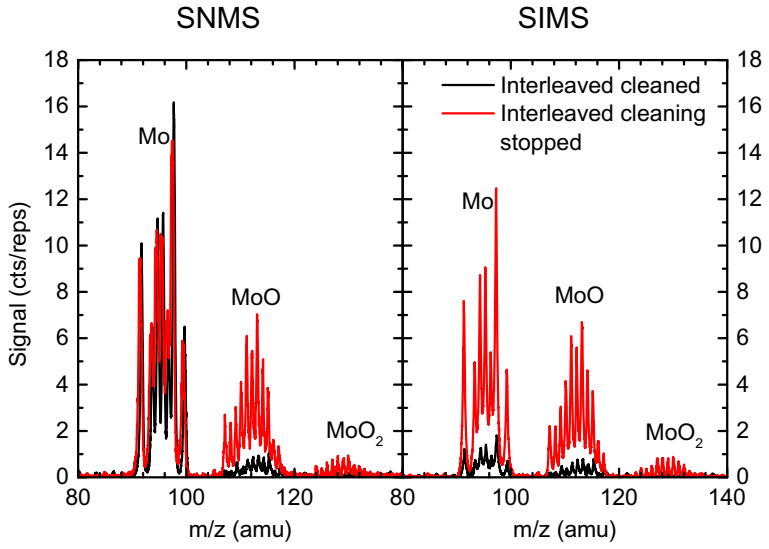

Fig. 3. SNMS and SIMS signal measured on a molybdenum surface bombarded with 5 keV Ar^+ ions with (black) and without (red) interleaved sputter cleaning. The signals in the left and right panels were obtained with and without firing the post-ionization laser, respectively. (For interpretation of the references to color in this figure legend, the reader is referred to the web version of this article.)

As will be shown below, the secondary ion signals of atoms sputtered from a clean metal surface are small compared to those of post-ionized neutrals under both bombarding conditions, yielding

$$\frac{\alpha_{MeV}^{+}}{\alpha_{keV}^{+}} \simeq \frac{S_0^{keV}}{S_+^{keV}} \cdot \frac{S_+^{MeV}}{S_0^{MeV}} \simeq \frac{S_{SNMS}^{keV}}{S_{SIMS}^{keV}} \cdot \frac{S_{SIMS}^{MeV}}{S_{SNMS}^{MeV}} \quad (4)$$

In the following, we will present the results of preliminary proof-of-principle experiments on dynamically cleaned elemental surfaces that were performed during two different beam time periods at the UNILAC. Since the methods and strategies for data acquisition at the UNILAC were dynamically developed during these periods, not all methods were already available when some of the data was taken.

3.1. Indium

The spectra measured on a dynamically cleaned polycrystalline indium sample are shown in Fig. 4. The spectrum displayed in the upper panel was taken with the 5 keV Ar^+ ion beam and shows the well known distribution of neutral indium atoms and clusters sputtered under these conditions [14]. The spectrum displayed in the center panel was measured with the UNILAC beam and shows a much smaller indium atom signal and no indication of sputtered clusters. Both spectra exhibit abundant signals in the low mass range as well as in the range between 200 amu and 350 amu. The spectrum in the bottom panel shows the result measured with both ion beams off, i.e. with the laser beam alone. It is apparent that particularly the signals detected at higher masses are caused by the photoionization of residual gas components present in the vacuum system. Depending on the history of previously performed experiments, such signals are sometimes observed at the UNILAC, while at other times the residual gas background is negligible (see below). We attribute this finding to the fact that the swift heavy ion beam may cause very large sputtering yields on some samples, which may lead to the deposition of material at the vacuum chamber walls which then evaporates during subsequent SHI beam irradiation. As a consequence, the level of residual surface contamination achievable under dynamic sputter cleaning conditions may vary from one experiment to the other, rendering the results of absolute ionization probability measurements somewhat questionable. One can, however, subtract the background spectrum from the two other spectra. A section of the resulting spectrum is shown in Fig. 5. It is seen that now the In_2, In_2O and In_2O_2 signals are clearly discernible in the Ar^+ induced spectrum, which in the original spectrum were completely masked by the residual gas background. In the SHI induced spectrum, In_2 is not detectable, but signals at In_2O and In_2O_2 can be identified. This finding shows that under swift heavy ion bombardment conditions the oxide signals must strongly dominate over the bare metal clusters, thereby suggesting that these signals may be caused by sputtering of remaining oxide patches on the surface. In fact, it is well known that band gap materials like oxides generally exhibit much higher SHI induced sputter yields than metallic samples [5], a finding which is in marked contrast to keV sputtering as seen in Fig. 4.

In order to determine the ionization probability of sputtered indium atoms, we employed the delay technique described above to allow the acquisition of secondary ion and post-ionized neutral data within the same TOF spectrum. The result is shown in Fig. 6, where the SNMS peaks corresponding to the m/z 113 and 115 isotopes of indium are marked by the grey and yellow areas, respectively. Note that in this case the secondary ion and post-ionization signals are separated in time, and therefore the SNMS signal does not represent the sum of S_0 and S_+ but rather allows to extract both signals simultaneously from the SNMS spectrum. The first observation is that secondary ion and post-ionized neutral signals exhibit different peak shapes, with the secondary ion peaks showing pronounced tails towards higher flight times. This finding is caused by the fact that the post-ionization laser does not homogenously illuminate the entire sensitive volume of the TOF spectrometer as depicted in the Supplementary information. While the detected secondary ions originate from the entire sensitive volume, post-ionized neutral particles can only be extracted from the (smaller) post-ionization volume determined by the laser focus. Analysis shows that the tails observed for the SIMS peaks originate from ions located above the center of the sensitive volume, i.e., closer to the extraction electrode, and therefore enter the field free drift region with a smaller kinetic energy leading to larger flight time. The peak shape observed for these ions therefore reflects the time refocusing properties of the TOF spectrometer. By comparing the spectra taken with and without the post-ionization

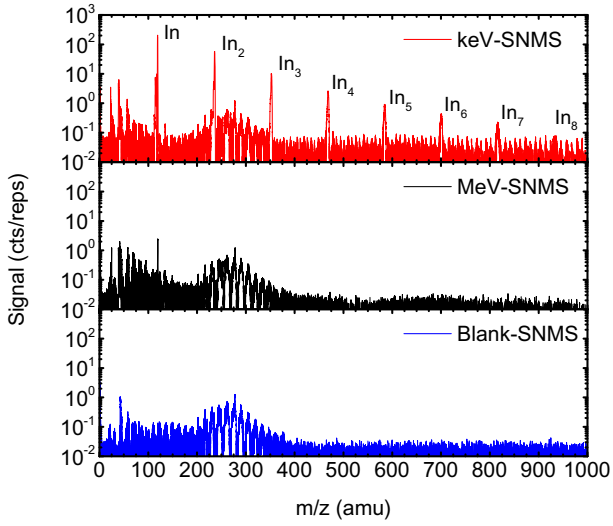

Fig. 4. SNMS spectra measured on a dynamically cleaned polycrystalline indium sample und bombardment with 5 keV Ar^+ (upper panel), 4.8 MeV/u Au^{26+} (center panel) and without ion bombardment (bottom panel).

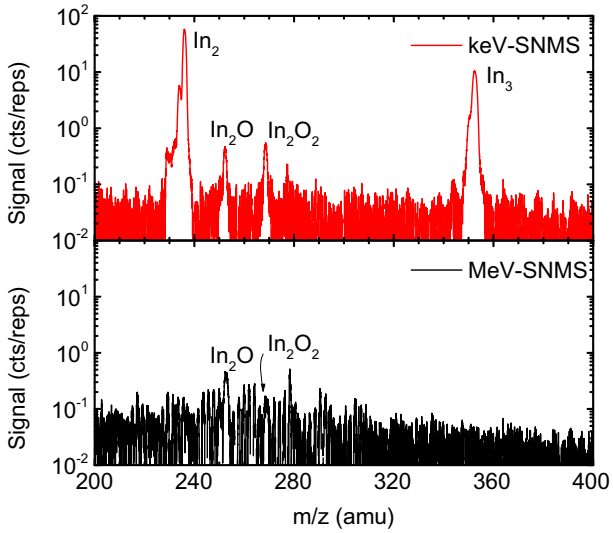

Fig. 5. Signal of post-ionized neutral indium atoms and indium oxide clusters sputtered from a clean polycrystalline indium surface under bombardment with 5 keV Ar^+ ions (upper panel) or 4.8 MeV/u Au^{26+} ions (lower panel) after residual gas background subtraction as described in the text.

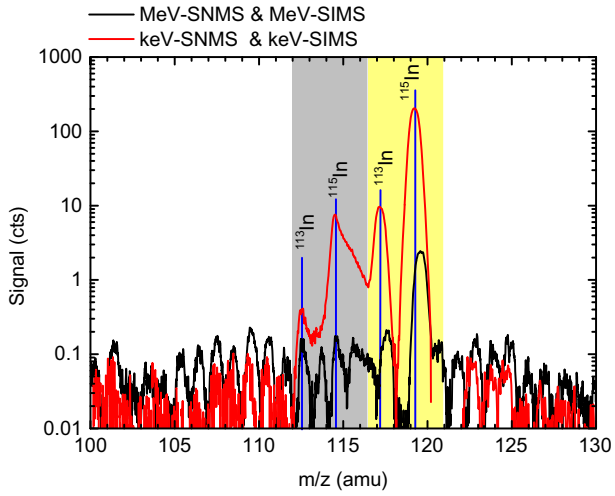

Fig. 6. Signal of post-ionized In atoms (yellow area) and In^+ secondary ions (grey area) sputtered from a dynamically cleaned indium surface under bombardment with 5 keV Ar^+ (red line) or 4.8 MeV/u Au^{26+} ions (black line), respectively. The secondary ion and post-ionized neutral spectra were displaced relative to each other using the delay technique described in the text. (For interpretation of the references to color in this figure legend, the reader is referred to the web version of this article.)

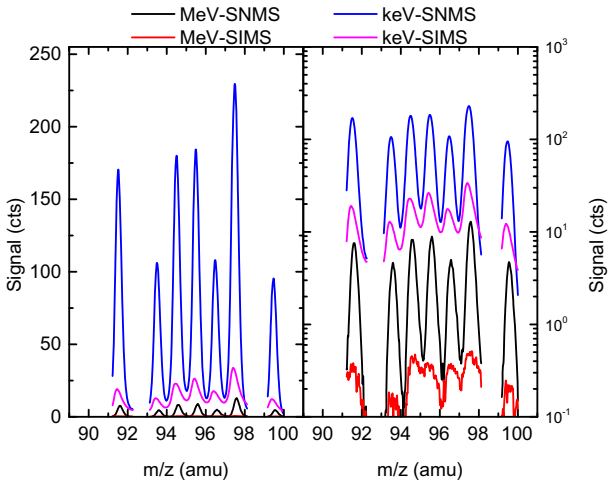

Fig. 7. SNMS and SIMS spectra of Mo atoms sputtered from a dynamically cleaned polycrystalline molybdenum surface under bombardment with 5-keV Ar^+ ions (labeled "keV") or 4.8 MeV/u Au^{26+} ions (labeled "MeV"), respectively.

laser, we note that the secondary ion peaks did not change upon blocking or unblocking the post-ionization laser, indicating that multiply charged ion formation via photoionization of secondary ions does not influence the measured signals.

As outlined above, the detected secondary ion and neutral signals can be used to determine the relative ionization probabilities under both bombarding conditions. As seen from Fig. 6, the secondary ion signal is sufficiently small compared to the post-ionized neutral signal to warrant the use of Eq. (4). We use the signals of the major m/z 115 isotope for the analysis, since the m/z 113 isotope signal acquired under SHI irradiation appears to be overlapped with a background signal. Since the $^{115}In^+$ signal is also close to the background level, we cannot exclude a possible background contribution to that signal as well. As a result, we therefore find $\alpha^+_{MeV} \leqslant (1.4 \pm 0.2) \times \alpha^+_{keV}$ for indium atoms sputtered under irradiation with 4.8 MeV/u Au^{26+} ions relative to 5 keV Ar^+ ions. It should be noted that this result may in principle be influenced by the residual surface contamination as mentioned above. Under the dynamic sputter cleaning conditions employed here, the state of the surface is determined by the balance between residual gas adsorption and dc sputtering with the 5 keV Ar^+ beam and, hence, likely to be independent of whether the keV or MeV ion beam is used for data acquisition. Although absolute values of the ionization probability are known to critically depend on the surface cleanliness, we therefore expect that this influence should be similar under both bombarding conditions, so that the relative ionization probability ratio determined here is presumably less influenced. For the same reason, the result obtained here is not influenced by the peak shape difference between secondary ion and neutral mass peaks as discussed above, since – as outlined in the discussion of Eq. (2) – the influence of an unsaturated post-ionization efficiency is the same under both bombarding conditions and therefore cancels in the relative ionization probability ratio.

3.2. Molybdenum

SNMS and SIMS spectra obtained on a dynamically cleaned molybdenum sample are shown in Fig. 7. It is seen that the isotopic abundance pattern of Mo atoms can be clearly identified under both bombardment conditions, ensuring that particularly the SIMS signals are not overlapped with significant background signal. In principle, it appears straightforward to apply Eq. (4) to calculate the relative ionization probability. The resulting apparent relative ionization probability ratio calculated for each isotope separately is displayed in Table 1. These data, however, need one further correction as follows.

When the interleaved data acquisition method depicted in Fig. 2 was first implemented, it was found that secondary ion spectra recorded during the UNILAC pulse exhibited varying intensities. In particular, it was discovered that the SNMS spectrum recorded when the post-ionization laser was blocked showed a different intensity than the interleaved SIMS spectrum recorded along with it. With the ionization laser blocked, however, both spectra should be identical, with the only difference being that they are taken at different times during an UNILAC pulse. Since the measured signal is directly proportional to the projectile ion current, we were forced to conclude that the UNILAC pulse must exhibit a non-rectangular temporal profile, where the momentary beam current varies as a function of time within one single pulse. In order to utilize the interleaved data acquisition technique described above, it is therefore mandatory to determine the pulse profile in order to normalize the spectra taken at different times to the momentary pulse current. We therefore developed a strategy to map the pulse profile by monitoring the SNMS signal as a function of time during the UNILAC pulse. For that purpose, the shot sequence was delayed in a controlled way with respect to the UNILAC pulse start and the Mo SNMS signal measured at each delay was integrated over all Mo isotopes and summed over 200 shots. The result is plotted in Fig. 8 and reveals a pronounced temporal variation of the SHI ion current throughout the pulse. In order to make sure that the characteristics of the UNILAC beam had not changed during the measurement, the spectrum corresponding to the first data point was measured again after completion of the entire series and found to coincide within a few percent. In the original interleaved data acquisition series, the SNMS spectrum is taken at the time marked by the red line, whereas the subsequent SIMS spectra were taken at the times marked by the blue lines. As a consequence, the measured intensities must be corrected by the average current measured at the blue lines relative to that measured at the red line. The resulting average value of the relative ionization probability ratio is $\alpha^+_{MeV}/\alpha^+_{keV} \leqslant (0.36 \pm 0.08)$ for Mo

Table 1
SNMS and SIMS signals of Mo atoms sputtered under bombardment of a dynamically cleaned molybdenum sample with 4.8 MeV/u Au^{26+} ("MeV") and 5 keV Ar^+ ("keV") ions, respectively, along with relative ionization probability calculated according to Eq. (4) in the text.

		Isotope						
		^{92}Mo	^{94}Mo	^{95}Mo	^{96}Mo	^{97}Mo	^{98}Mo	^{100}Mo
keV	SNMS	8757	5396	9441	9559	5541	12314	4422
	SIMS	1551	1022	1911	2077	1448	2699	999
MeV	SNMS	334	199	378	381	224	567	189
	SIMS	31	16	40	33	29	46	10
$\alpha^+_{MeV}/\alpha^+_{keV}$		53% (43 ± 10)%	42%	52%	40%	50%	37%	24%

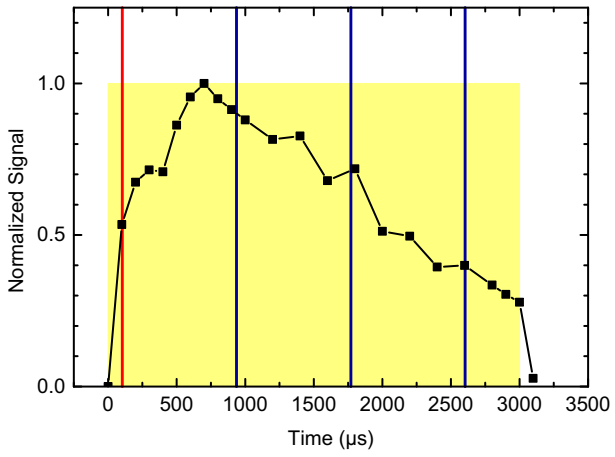

Fig. 8. Time dependence of Mo SNMS signal measured under bombardment of a dynamically cleaned molybdenum surface irradiated with 4.8 Mev/u Au^{26+} ions. The data were acquired at different times after the start of the ion pulse. The vertical lines indicate the time at which the SNMS spectrum (red line) and the SIMS spectra (blue lines) were taken. (For interpretation of the references to color in this figure legend, the reader is referred to the web version of this article.)

atoms sputtered from a dynamically sputter cleaned molybdenum surface under irradiation with 4.8 MeV/u Au^{26+} ions relative to 5 keV Ar^+ ions. For the case of molybdenum, the ionization probability under 5 keV Ar^+ ion bombardment was measured previously using the same TOF spectrometer as used here in connection with a more powerful laser installed in our lab. Using the value of

$$\alpha^+_{keV} = 1.1 \times 10^{-4}$$

determined there, we find

$$\alpha^+_{MeV} = (4.0 \pm 0.9) \times 10^{-5}$$

for molybdenum atoms sputtered from the dynamically sputter cleaned molybdenum surface under irradiation with 4.8 MeV/u Au^{26+} ions.

4. Conclusions

The present work provides a direct measurement of mass resolved ionization probabilities under Swift Heavy Ion bombardment conditions. Probably the most important result of the study is the observation that the ionization probability of atoms ejected from clean metal surfaces under electronic sputtering conditions appear to be similar to those observed in keV sputtering experiments. The relative (MeV/keV) ionization probabilities determined for dynamically sputter cleaned indium and molybdenum are both of the order of unity, with only small differences between both metals. This finding is interesting, since the absolute values of the ionization probabilities are very small (of the order of $10^{-5}\cdots10^{-4}$) and known to be extremely sensitive to surface contamination. The implication of this observation is twofold. First, the dynamical cleaning protocol invoked here apparently ensures sufficiently clean surface conditions which allow a reproducible assessment of the relative ionization probability ratio under SHI and keV ion bombardment conditions. Second, and more importantly, the data indicate that the mechanisms leading to the ionization of a sputtered atom must be similar. In a number of recent studies, we have modeled the secondary ion formation process particularly of atoms sputtered from a clean metal surface and concluded that the ionization is primarily governed by the temporal electronic excitation induced even by a keV ion impact, where the dominant mechanism slowing down the primary ions is nuclear stopping [15]. More specifically, it was found [16] that more than 50% of the initial kinetic impact energy of a 5 keV projectile may become temporarily deposited into the electronic system of the solid, where it manifests in form of electronic excitations which determine the charge state of an outgoing atom. In the electronic sputtering regime explored here, the primary energy deposition mechanism is via electronic excitation, fueling the expectation that ionization probabilities may be higher than under keV sputtering conditions. However, one needs to keep in mind that the time scale of primary excitation and particle emission are rather different. In fact, particle emission is believed to occur as a consequence of lattice heating via electron phonon coupling, which occurs on a time scale of the order of picoseconds after the projectile impact. At these times, electron and phonon temperatures have largely equilibrated, leading to similar values of the electron temperature as observed under keV bombardment conditions. Therefore, the observation made here may be not as surprising as it seems at first glance.

Acknowledgment

The authors are greatly indebted to the German Ministry of Science (BMBF) for financial support in the framework of the "Verbundprojekt 05K2013 – Ion Induced Materials Characterization and Modification".

Appendix A. Supplementary data

Supplementary data associated with this article can be found, in the online version, at http://dx.doi.org/10.1016/j.nimb.2015.07.117.

References

[1] M.L. Yu, Charged and excited states of sputtered atoms, in: R. Behrisch, K. Wittmaack (Eds.), Sputtering by Particle Bombardment III, Springer, Berlin, 1991, pp. 91–160.
[2] A. Benninghoven, F.G.R. Denauer, H.W. Werner, Secondary Ion Mass Spectrometry: Basic Concepts, Instrumental Aspects and Trends, Wiley, New York, 1987.

[3] Z. Sroubek, Formation of ions in sputtering, Spectrochim. Acta B 44 (1989) 317–328.
[4] A. Wucher, Formation of atomic secondary ions in sputtering, Appl. Surf. Sci. 255 (2008) 1194.
[5] W. Assmann, M. Toulemonde, C. Trautmann, Electronic sputtering with swift heavy ions, in: R. Behrisch, W. Eckstein (Eds.), Sputtering by Particle Bombardment, Springer, Berlin, 2007, pp. 401–450.
[6] M. Toulemonde, W. Assmann, C. Trautmann, F. Grüner, Jetlike component in sputtering of LiF induced by swift heavy ions, Phys. Rev. Lett. 88 (2002) 057602.
[7] H. Hijazi, H. Rothard, P. Boduch, I. Alzaher, F. Ropars, A. Cassimi, J.M. Ramillon, T. Been, B.B. d'Etat, H. Lebius, L.S. Farenzena, E.F. da Silveira, Interaction of swift ion beams with surfaces: Sputtering of secondary ions from LiF studied by XY-TOF-SIMS, Nucl. Instrum. Methods B 269 (2011) 1003–1006.
[8] F. Meinerzhagen, L. Breuer, H. Bukowska, M. Herder, M. Bender, D. Severin, H. Lebius, M. Schleberger, A. Wucher, Review of Scientific Instruments, submitted (2015).
[9] A. Wucher, M. Wahl, H. Oechsner, Sputtered neutral silver clusters up to Ag_{18}, Nucl. Instrum. Methods B 82 (1993) 337–346.
[10] M. Wahl, A. Wucher, VUV photoionization of sputtered neutral silver clusters, Nucl. Instrum. Methods B 94 (1994) 36–46.
[11] A. Wucher, Laser postionization – fundamentals, in: J.C. Vickerman, D. Briggs (Eds.), TOF-SIMS: Materials Analysis by Mass Spectrometry, IM Publications and SurfaceSpectra, 2013, pp. 217–246.
[12] A. Wucher, R. Heinrich, C. Staudt, A method for quantitative determination of secondary ion formation probabilities, in: A. Benninghoven, P. Bertrand, H.N. Migeon, H.W. Werner (Eds.), Secondary Ion Mass Spectrometry (SIMS XII), Elsevier Science, 1999, pp. 143–146.
[13] D. Koch, M. Wahl, A. Wucher, Electron impact and single photon ionization cross sections of neutral silver clusters, Z. Phys. D 32 (1994) 137–144.
[14] C. Staudt, A. Wucher, Generation of large indium clusters by sputtering, Phys. Rev. B 66 (2002) 075411–075419.
[15] A. Wucher, B. Weidtmann, A. Duvenbeck, A microscopic view of secondary ion formation, Nucl. Instrum. Methods B 303 (2013) 108–111.
[16] A. Wucher, A. Duvenbeck, Kinetic excitation of metallic solids: progress towards a microscopic model, Nucl. Instrum. Methods B 269 (2011) 1655–1660.